eleventh
NAMC
minneapolis, mn usa

j u n e 5 – 8 2 0 1 1

IN-PLANE BEHAVIOR OF TUFF MASONRY PANELS STRENGTHENED WITH FRP DIAGONAL LAYOUT

Giancarlo Marcari[1], Daniel Oliveira[2], Giovanni Fabbrocino[3] and Paulo B. Lourenço[4]

Abstract

The present paper deals with a quantitative analysis of the shear strength behavior of masonry panels strengthened with diagonal layout. The objective of the study is to progress towards understanding the shear strength contributions from masonry and FRP to the lateral resistance of strengthened panels. To this aim, relevant experimental results of monotonic shear-compression tests are analyzed. The local behavior of the reinforcement is investigated in terms of FRP strain profiles (i.e. the transferrable tension force within FRP), and its effects on the global response of the panels assessed. The experimental results show the effectiveness of the anchorage system in restraining the FRP at the anchored edges, avoiding premature failure due to FRP debonding. As a result, the specimens were allowed to develop their full lateral resistance. A truss model approach, combined with a proper masonry strength criterion for masonry is proposed and validated. A comparison between computed and experimental data confirms the validity of the procedure in view of practical applications and code recommendations.

Keywords: masonry, shear, composite materials, FRP strains, FRP diagonal layout

---

[1] Assistant Professor, ISISE, University of Minho, Dept. of Civil Eng., 4800-058, Guimarães, Portugal, marcarigiao@civil.uminho.pt
[2] Assistant Professor, ISISE, University of Minho, Dept. of Civil Eng., 4800-058, Guimarães, Portugal, danvco@civil.uminho.pt
[3] Associate Professor, Strega Lab., University of Molise, 86039, Termoli, Italy, giovanni.fabbrocino@unimol.it
[4] Full Professor, University of Minho, ISISE, University of Minho, Dept. of Civil Eng., 4800-058, Guimarães, Portugal, pbl@civil.uminho.pt

Introduction

In the past two decades, the use of externally bonded fiber reinforced polymer (FRP) composites has steadily increased as an efficient technique for structural retrofitting and seismic reinforcement of masonry components. The response of FRP-strengthened masonry has extensively been studied both experimentally and numerically with an emphasis on overall shear capacity, ductility, and failure modes. A recent comprehensive literature survey on experimental works can be found in the ACI 440.7R-10 [2010] guide.

Although significant progress in knowledge has been made, there is a critical need for the development of design provisions for FRP diagonal layouts.

Various theoretical models based on truss mechanisms have been proposed in order to compute the contribution of the diagonal FRP reinforcement to shear resistance of panels [Prota 2008, Zhao 2003]. However, with the exception of [Stratford 2004], masonry shear strength enhancement due to the truss mechanism has not been taken into consideration, thereby neglecting the crucial aspect related to the synergistic interaction between FRP and masonry. In this regard it is noted that the recent guidelines [ACI 440.7R-10 2010, CNR-DT 200/2004 2008] still do not enclose design expressions for FRP diagonal configurations. Substantial knowledge gaps that still need to be filled for diagonal FRP layouts include: (i) a link between local (FRP–masonry interfacial) behavior and global response of the panels, (ii) a quantitative analysis of shear contributions from both masonry and FRP reinforcement and (iii) development of suitable bond strength models for different types of masonry substrate.

The present paper focuses on the experimental behavior of masonry panels strengthened with FRP diagonal configuration. To this aim, the experimental test results of tuff masonry panels with FRP layout obtained by [Marcari 2007] have been selected. The objective is to provide additional experimental data with reference to the local strain behavior of the diagonal reinforcement, and the quantitative evaluation of the weight given to masonry and FRP shear strength contribution to lateral resistance of the strengthened panels. The local FRP strain readings allowed to investigate the debonding process of both compressed and tensioned plies, and its effects on the shear response and lateral deformation of the panels. The role of the anchorage system on the experimental local and global behavior of the panels is also investigated. An analytical study on the strength contributions from masonry and FRP is carried out using a truss model approach, combined with a proper shear strength model for masonry. From comparisons between computed and experimental data, relevant results are presented and discussed.

# Experimental campaign: brief review of the shear-compression tests

The experimental campaign carried out by some of the authors since 2007 is analyzed. Test layout and results are extensively reported elsewhere [Marcari 2007], but in the following some aspects of the experimental program are herein briefly revisited.

The tests were performed on multiple leaf tuff masonry panels having dimensions of 1570 x 1480 x 530 mm with partial connection between the external leaves. Shear loading was applied under displacement control once the axial load (N_o) was imposed. The reinforcement consisted of diagonal 200 mm wide FRP plies bonded on the two sides of the panel as shown

in Figure 1a. Two composite materials were used, namely CFRP and GFRP. Moreover, the test variables included the FRP amount, i.e. one layer (LD) and two layers (HD) for each diagonal ply. The FRP-strengthened panels are denoted by a code where the first letter is C or G depending whether CFRP or GFRP, followed by LD or HD depending on the number of FRP layers. Finally, the alphabetic letters "a" or "b" are used to indicate the two specimens with identical FRP reinforcement which were tested for each diagonal layout (with the exception of LD GFRP). A total of 4 unstrengthened panels and 7 strengthened specimens were tested. As for the strengthened specimens, the programme was as follows: two panels with LD CFRP (CLDa and CLDb); two panels with HD CFRP (CHDa and CHDb); one panel with LD GFRP (GLD) and two panels with HD GFRP (GHDa and GHDb).

The diagonal plies were anchored at the edges thorough horizontal FRP plies either wrapped around the panel section, or partially-wrapped (called herewith U-wrap), as schematically illustrated in Figure 1b. The latter system was used for specimens CHDa and GHDa. The FRP material properties are given in [Marcari 2007].

The specimens were extensively instrumented. The FRP reinforcement strains were measured using 5 mm gauge-length strain gauges (SGs), with a measurement range limited to ±5000 με. The measurement points are shown in Figure 1a. Symmetry of the gauge points was ensured on the two sides of the panel. Typically, only one side of the panels was gauged completely (i.e. side A). Panels CHDa and GHDa were instrumented with SGs on both sides.

The experimental program included also compression tests of the unstrengthened panels. The average compressive strength was equal to 1.1 MPa (CoV=27%), and the elastic modulus was equal to 635 MPa (CoV=8%).
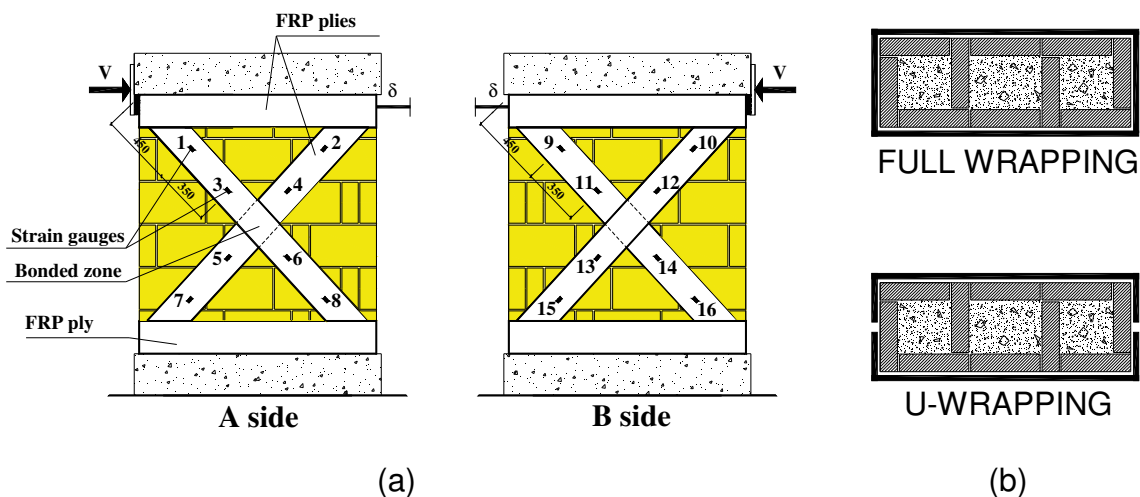

Figure 1. (a) FRP shear strengthening; (b) anchorage system of the diagonal plies

The shear response of unstrengthened panels was governed by the formation and development of inclined diagonal cracks, which propagated through mortar joints and stones. The average maximum lateral resistance (V_{max}) approached 132 kN with CoV equal to 26 %. All strengthened panels failed in shear, characterized by the formation of diagonal cracks, with vertical cracks occurring on the lateral compressed side, accompanied normally by spalling of the external stones.

The shear force vs. horizontal displacement curves (V-δ) are reported in Figure 2. This figure illustrates also the V-δ curves obtained for the unstrengthened panels. It is worth noting that all V-δ curves are plotted up to collapse of the panels. Details about the displacement capacity of the strengthened panels can be found in [Marcari 2007].
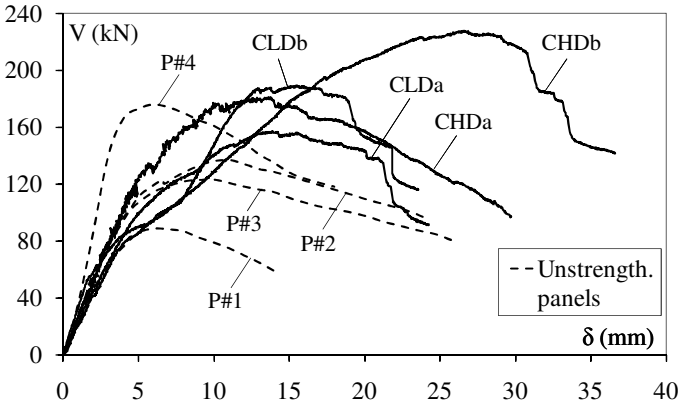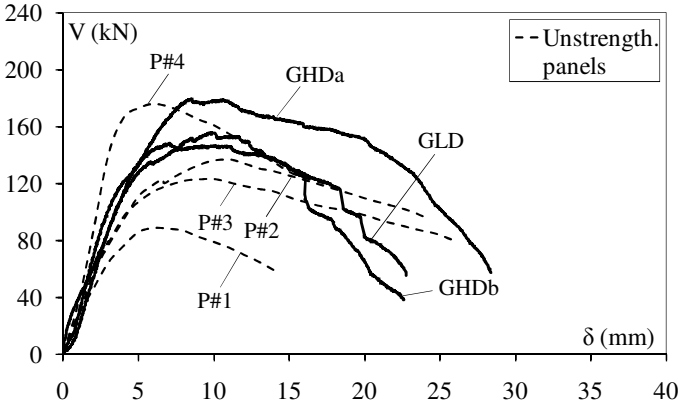
Figure 2. Comparisons of experimental shear force-horizontal displacement curves: (a) CFRP and (b) GFRP

Behavior of FRP strains

The experimental strain vs. horizontal displacement curves (strain profiles) monitored along the diagonal plies are used to investigate the effect of the local (interfacial) behavior of the FRP on the global response of the panels, focusing on debonding of the FRP from the substrate, as well as on the average peak strains within FRP. It is noted that debonding of FRP from the substrate is intended not as peeling failure (which involves direct tensile stress), but as shear delamination failure. The results are presented for panels CHDa and GHDa which were gauged on the two sides.

Panel CHDa

The strain profiles from side A of the panel are illustrated in Figure 3a. It can be observed that the strain profiles on the opposite sides of the wall followed a similar trend.

The readings on side A started with an average strain level of -315 µε, while those on B side started with an average of -375 µε, due to the pre-compression load applied to the panel.

The local debonding of the compressed ply on side A and B initiated above the central zone of the wall at a δ = 5.0 mm (drift=0.35%), as it was detected by the strain readings of SG #1 and #3 on side A (Figure 3a), and SGs #10 and #13 on side B. The average debonding strain ranged between -700 µε and -1100 µε. At this point, the lateral shear force was approaching 130 kN on the ascending branch, about 70% of the wall peak load. The part of the compressed plies below the central zone of the panel locally debonded at δ = 9.5 mm (drift=0.6%), for an average strain of about -1100 µε, as shown by SG #6 and #8 on A side. At this point the lateral resistance of the wall was close to its peak value. After this displacement the compressed plies started to buckle locally (Figure 3a).

As for the tension plies, the pairs SG #5 and #14, and SG #7 and #16, placed symmetrically on the two sides of the walls showed higher strain values since the onset of the test (Figure 3b). The drops of strain occurred at a δ = 16.2 mm (drift =1.0%) on side A, and at δ = 13.5 mm (drift=0.86%) on side B were due to a sudden debonding of the tensile plies from the substrate (see Figure 3b). The debonding occurred for a lateral resistance decay of 8% or lesser (Figure 3c). The maximum tensile strains occurred at δ = 21.1 mm (drift=1.3%), when the lateral resistance reduced of about 8% on the V-δ descending branch. The values approached +2630 µε and +2995 µε on side A and B, respectively. The maximum tensile strain value, averaged from both sides of the panel was 2810 µε.

Panel GHDa

The strain-lateral displacement curves on side B of the panel are illustrated in Figure 4. Once again it was found that the strain profiles from both sides behaved in a similar manner. The strain readings started with negative values due to the initial pre-compression loading. The average compressive deformation approached -228 µε on A side, and -180 µε on B side.

Cracks in the masonry initiated at about δ = 5 mm (drift=0.3%), and about 70% of the peak load. This led to a reduction of stiffness in the global behavior, as can be seen in Figure 4c. At this point, the strain profiles showed a change in slope, with an increase of stiffness. The compressed plies initiated to debond below the central zone of the panel at about 8.0 mm (drift=0.6%), when the lateral peak force was attained. This behavior can be detected from the strain readings of SG #6 and #8 on side A, and from SG #13 and #15 on side B (Figure 4a). The compressed plies resulted fully debonded at around δ =13 mm (drift=0.86%) when the V-δ curve was approaching the softening branch (see Figure 4a and Figure 4c). After that displacement, the plies buckled locally.

The debonding strains of the compressed plies ranged between -810 µε and -950 µε. The strains measured below the centre line of the wall stayed relatively high, as shown by SG #5 and #14, as well as by SG #7 and #16. In correspondence of the peak lateral resistance, the readings of SGs #7 and #16 exceeded the limit of +5000 µε (Figure 4b). However, no fracture of the FRP reinforcement was observed.

The experimental curves of SG #2, #4, #5 on side A, and SG #9, #11, #14 on side B indicate that the maximum tensile strains are attained when the lateral load resistance drops by about 25%-30%, with δ = 20-25 mm (drift=1.3%-1.6%). At that displacement, the panel was characterized by vertical cracks that developed across stones and mortar joints at the compressive side of the panel, which caused spalling of the lateral stones.

Discussion of the experimental results

Behavior of the tested panels

Based on the test results, the behavior of the strengthened panels upon increasing lateral displacement can be investigated. The panels were initially in an uncracked state, and the FRP was fully bonded and acted compositely with the masonry. The initial lateral stiffness of the strengthened panels was not significantly influenced by the FRP. In fact, no relevant differences have been found between the stiffness of the unstrengthened and strengthened panels before cracks in the strengthened masonry caused the change of slope of the V-δ curve (Figure 2). Upon increasing lateral displacement, local FRP debonding occurred which typically started propagating from the centre of the panels.

Debonding of the compressed plies developed in the pre-peak regime of the panels. Let $\xi_{deb}=V_{deb}/V_{max,exp}$ be the ratio between the lateral force at the debonding of the compressed plies (V_{deb}), and the peak load ($V_{max,exp}$). The wall lateral drifts and the ξ_{deb} ratios experienced by the panels at debonding of the compressed plies are summarized in Table 1. From this table it can be seen that the compressed plies debonded when the lateral force was on the ascending branch of the V-δ curve, ranging between levels of 70% and 100% of the peak load. However, the lateral drift at which debonding of compressed plies occurred seems not to be correlated with the FRP type or FRP amount (values ranged between 0.25% and 0.90%).

As for the tensile plies, the strain profiles showed a non linear behavior, characterized by an irregular path around the peak lateral force, when major cracks were developing across masonry.

The lateral drifts attained in correspondence of the maximum tensile strains (ε_{max}) in the FRP have been summarized in Table 1. The lateral drift averaged 1.5% in the case of CFRP reinforcement, while it varied from 0.90% to 1.60% in the case of GFRP reinforcement.

The last column of Table 1 gives the reduction of lateral strength in correspondence of ε_{max} calculated as $S_r = V_{\varepsilon,max} / V_{max,exp}$, where $V_{\varepsilon,max}$ is the lateral force that corresponds to $\varepsilon_{max.}$

It was observed that the peak values of the tensile strains occurred in correspondence of the softening branch of the V-δ curves. At that stage, the walls were severely cracked and the diagonal tensile plies debonded from the substrate. However, the diagonal tension action through the FRP was still reacted by a vertical compression in the masonry until the anchorage system peeled off from the support, or the panel spalled on its compressive side.
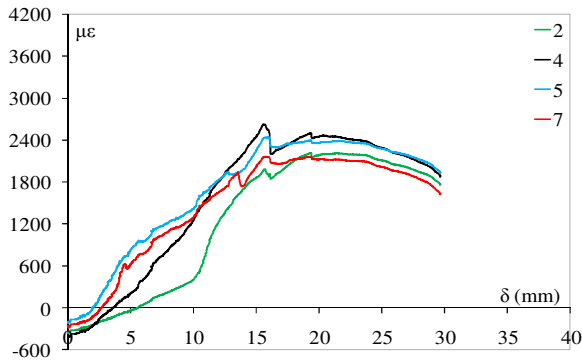
An important phenomenon that has been found in the behavior of panels CHDa and GHDa is that the strains readings on both sides of the specimens displayed substantial symmetric profiles. In practice, the debonding and peak strains occurred under the same lateral drifts.
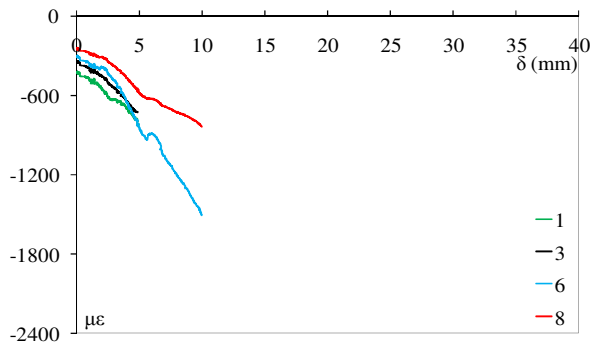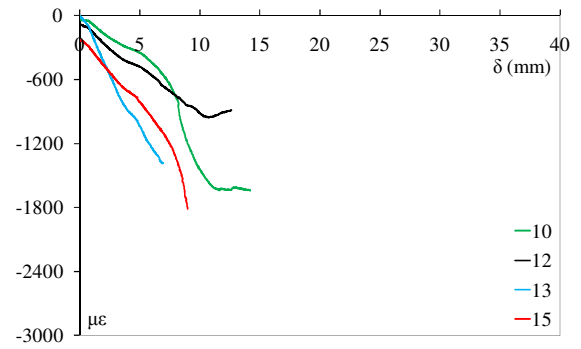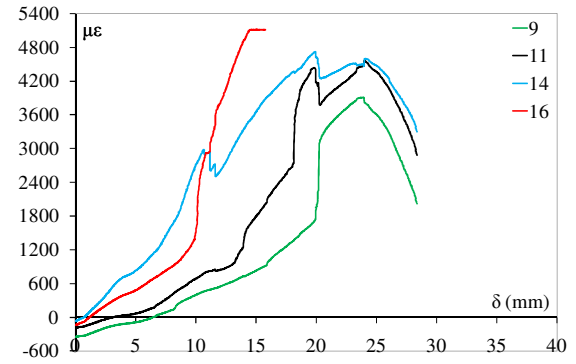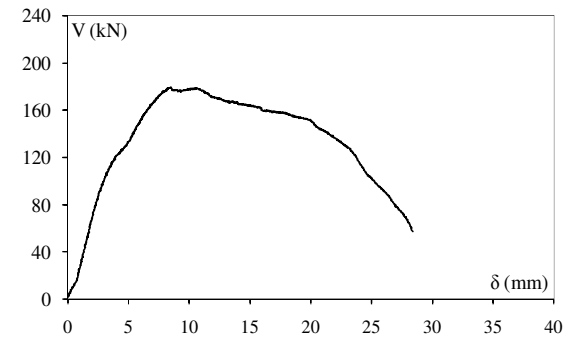
Figure 3. Panel CHDa: compressive (a) and tensile (b) strain profiles on side A; (c) V-δ curve

Figure 4. Panel GHDa: compressive (a) and tensile (b) strain profiles on side B; (c) V-δ curve

Table 1. Experimental drifts and lateral force at the debonding of the compressed plies for the maximum tensile strains

Panel label	At debonding of the compressed plies		At the maximum tensile strain	
	Panel lateral drift	ξ_{deb}	Panel lateral drift	S_r
	(%)	(%)	(%)	(%)
CLDa	0.50 ÷ 0.65	70 ÷ 85	1.40	15
CLDb	0.75 ÷ 0.80	85 ÷ 90	1.30	10
CHDa	0.35 ÷ 0.60	70 ÷ 100	1.30	20
CHDb	0.75 ÷ 0.80	70 ÷ 75	1.90	10
GLD	0.45 ÷ 0.50	80 ÷ 100	1.00 ÷ 1.15	20 ÷ 25
GHDa	0.80 ÷ 0.90	95 ÷ 100	1.30 ÷ 1.60	25 ÷ 30
GHDb	0.25 ÷ 0.45	75 ÷ 100	0.90	11

It was observed that the lateral displacement of the panel caused direction changes in the diagonal tensile plies (see Figure 5a and Figure 5c). As a consequence, the tensile force was not perfectly centered along the ply length, and introduced locally a bending moment which lead, in the case of the lower strength FRP type (i.e. GFRP), to the rupture of the ply as in the case of GLD (Figure 5c) and GHDb. Moreover, FRP rupture generally occurred below the horizontal centre line of the wall, between SG #5 and SG #7, when the lateral strength reduced between 20% and 25% on the softening branch.
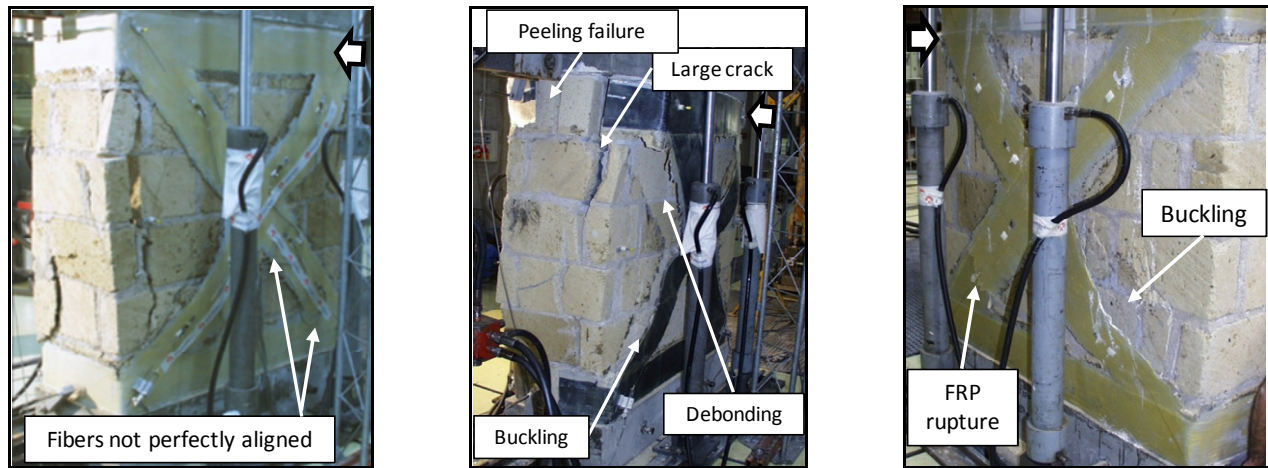
(a) Damage at 1.4% drift on side A

(b) Damage at 1.90% drift on side B

(c) Damage at 1.2% drift on side A

Figure 5. Damage of selected strengthened panels: (a) GHDa; (b) CHDb; (c) GLD

Role of the anchorage system

From the experimental tests it emerges that the two anchorage systems envisaged in the study resulted effective in preventing premature failures through peeling-off of the FRP strengthening at the anchored edges. As a result, the full shear capacity of the masonry panels was developed. Panels CHDa and GHDa with full wrapping anchorage, showed a less strength degradation than specimens CHDb and GHDb characterized by the U-wrap anchorage, as seen in Figure 2. The U-wrap anchorage system affected the failure mode of the panels. In fact, relevant cracks that developed along the compressed lateral side of the panels were basically triggered by the U-wrap anchorage. The splitting was generally accompanied by spalling of lateral stones as illustrated in Figure 5b. However, the experimental results indicated that this failure led to a rapid loss of strength and stiffness of the panels when the lateral resistance reduced by 10%-15%. In this situation the diagonal reinforcement was no longer able to transfer any load to the masonry in a controlled manner.

Analytical investigation

Analysis of FRP contribution to shear capacity

In this section, following an approach similar to that used by [Stratford 2004], a truss-based model shown schematically in Figure 6 is used in order to evaluate the shear contribution due to the external shear reinforcement (V_{frp}) and the increased vertical load in the masonry ($N_{m,frp}$). Basically, in this model the shear carrying mechanism associated with the FRP reinforcement is characterized by a vertical masonry compression strut and a diagonal FRP tension tie.
Therefore, the tensile force in the diagonal plies (F_{frp}) is computed from the experimental strain profiles $\varepsilon_{frp}(\delta)$ as follows:

$$F_{frp}(\delta) = n \times (E_{frp} \times w_{frp} \times t_{frp}) \times \varepsilon_{frp}(\delta) \qquad \textbf{[1]}$$

with n = FRP ply number; E_{frp} = elastic modulus of the FRP; w_{frp} and t_{frp} = width and thickness of the diagonal ply, respectively.
It is worth noting that the strain profile $\varepsilon_{frp}(\delta)$ in Equation 1 is the 'average profile' of the family of tensile strain curves plotted for a single panel side, with the exception of panels CHDa and GHDa where $\varepsilon_{frp}(\delta)$ is the average of the tensile strain profiles along both sides of the specimens.
The contribution from the FRP to the shear strength is computed from the horizontal equilibrium of the node point P:

$$V_{frp}(\delta) = F_{frp}(\delta) \times \cos\theta \qquad \textbf{[2]}$$

where θ is the angle between the ply and the horizontal direction. From the vertical equilibrium, the vertical load carried through the masonry by truss mechanisms results as follows:

$$N_{m,frp}(\delta) = F_{frp}(\delta) \times \text{sen}\theta \tag{3}$$
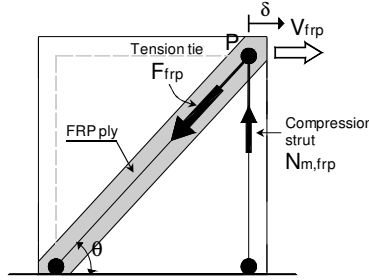
Figure 6. Adopted truss model

Figure 7 presents the values of V_{frp} as a function of the displacement δ for all tested panels, together with two V-δ curves representative of the lower and upper curve in the behavior of the unstrengthened panels.

The figures show that $V_{frp}(\delta)$ is characterized by an approximately linear behavior, followed by a nonlinear path as the V-δ diagram of the strengthened panels approach the peak load. Comparing the curves plotted in Figure 7, it is interesting to note that the peak of V_{frp} and the peak of the (V-δ) curves of the unstrengthened panels occurred for different lateral displacement. In particular, the shear strength from masonry without FRP is achieved at a lower lateral displacement than the shear strength from FRP. Moreover, when fully wrapping anchorage was used (i.e., panels CHDa and GHDa), the post-peak of the V_{frp}-δ diagram exhibited softening behavior (Figure 7).

Analysis of shear strength contribution of masonry

Test results are used to compare shear strength equations proposed in literature, respectively associated to diagonal tension shear failure and rocking failure mechanism. The shear strength associated to sliding mechanism is neglected because no experimental evidence of sliding failure was detected. The diagonal tension shear strength can be computed with a shear strength formulation originally derived by [Turnšek 1971], and largely adopted in design and assessment of masonry structures [NTC 08 2008, Magenes 1997] in the form:

$$V_{m,diag.shear} = B \cdot t \cdot \frac{1.5\tau_{od}}{b} \sqrt{1 + \frac{\sigma_o}{1.5\tau_{od}}} \qquad b = \frac{H}{B}; \ 1 \le b \le 1.5 \tag{4}$$

where B is the base, H the height and t the thickness of the panel; σ_0 = N/A is the average stress on the gross section area A; τ_{od} the diagonal shear strength of masonry.

The maximum shear associated to flexural mechanism is calculated according to NTC 08:

$$V_{m,flexural} = \psi \cdot \frac{B^2 \cdot t}{H} \frac{\sigma_o}{2} \left(1 - \frac{\sigma_o}{0.85f_m}\right) \tag{5}$$

where H is the wall height, f_m is the compressive strength of masonry, and ψ is a parameter which describes the boundary conditions, taking a value of 2 for fixed-ended wall.

In absence of experimental tests in order to evaluate τ_{od}, recommended values by building codes or available databases can be taken into consideration. Therefore, the value τ_{od}=0.038 MPa has been selected from literature works [Db Murature Unina-DIST 2009]. The choice to use that value of τ_{od} results in good agreement with the values recommended by the Italian building code NTC 08.

By assuming the vertical load N equal to the average precompression load (N_o) in the wall, the values of the shear resistance $V_{m,No}$ of the unstrengthened masonry calculated in compliance with Equation 4 have been reported in Table 2.
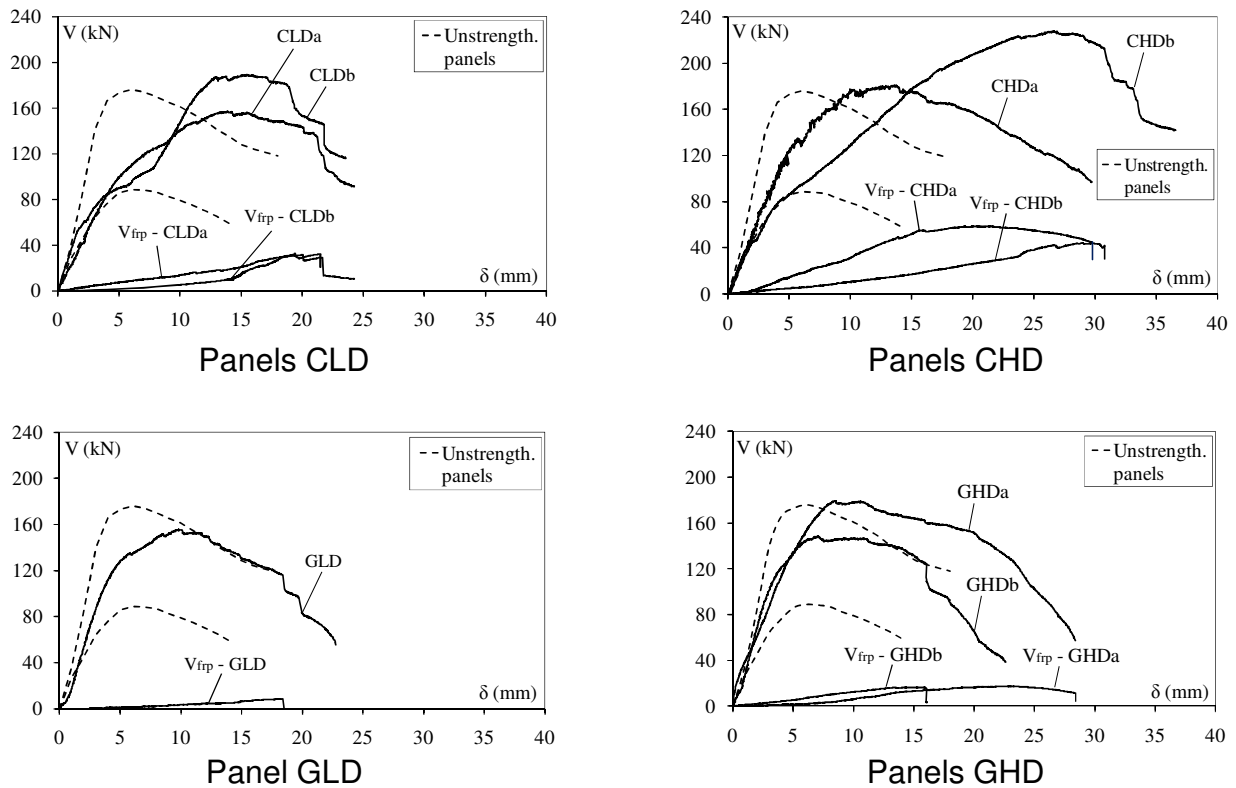
Figure 7. Experimental V-δ curves and computed shear strength contribution from FRP

The computed $V_{m,No}$ averaged 130kN, and the ratio $V_{m,No}/V_{max,exp}$ approached the value of 1 with associated CoV=29%. In the case of flexural failure (Equation 5) the shear strength approached 172 kN. Therefore, good agreement between the result of Turnšek and Căcŏvič's expression and the experimental strength is found. Based on this result, and considering that the strengthened masonry walls failed typically in diagonal shear, Equation 4 will be used to predict the masonry contribution to shear resistance of the reinforced panels. The validity of this assumption will be discussed in the next section.

Validation of the theoretical model

The experimental shear strength of the strengthened panels is computed with Equation 6:

$$V_{SM} = V'_m + V_{frp} \qquad\qquad\qquad\qquad [6]$$

where V'_m is the shear strength of masonry computed for the increased vertical load $N_o + N_{m,frp}$ due to truss mechanism. In the following analysis the maximum values of the functions $F_{frp}(\delta)$, $V_{frp}(\delta)$ and $N_{m,frp}(\delta)$ have been considered. Accordingly, the shear strength V'_m in Equation 6 has been estimated with Equation 4, assuming $N=\max(N_o + N_{m,frp})$.

The computed values $N_{m,frp}$, V_{frp} and V'_m, the sum V_{SM}, the ratio $V_{SM}/V_{max,exp}$ of predicted value to the experimental value have been reported in Table 2.

The results indicate that Equation 6 seems to provide a good and (slightly conservative) estimate of the capacity of the FRP-strengthened panels. Therefore, the adoption of Equation 4 in predicting masonry shear strength of the strengthened specimens is possible. The weight of the contributions from masonry and FRP to the lateral shear resistance of the strengthened panels has been evaluated by calculating the ratios $V_{frp}/V_{max,exp}$, and $V'_m/V_{max,exp}$. The results are reported as a percentage of $V_{max,exp}$ in Table 2.

It was found that the FRP contribution is larger in the case of panels strengthened with CFRP (25% for panels CHD) and lower in the case of panels with GFRP (6% for panel GLD). Moreover, the contribution of FRP increased about 50% from panels CLD to panels CHD, and about 65% from GLD to GHD. Also, the contribution of the reinforcement in the case of CLD panels is about 180% greater than that of GLD, while the contribution in the case of CHD was about 160% greater than that of GHD.

Table 2. Results and comparisons between experimental and calculated shear strength contributions

Specimens	Exp.data		Computed values					Comparative analysis		
	N_o	$V_{max,exp}$	$N_{m,frp}$ (Eq. 3)	$V_{m,No}$ (Eq. 4)	V_{frp} (Eq. 2)	V'_m (Eq.4)	V_{SM} (Eq. 6)	$\dfrac{V_{SM}}{V_{max,exp}}$	$\dfrac{V'_m}{V_{max,exp}}$	$\dfrac{V_{frp}}{V_{max,exp}}$
	(kN)	(kN)	(kN)	(kN)	(kN)	(kN)	(kN)	(-)	(%)	(%)
P#1	384	91.8	-	130.1	-	-	-	-	-	-
P#2	381	136.7	-	129.7	-	-	-	-	-	-
P#3	388	123.0	-	130.7	-	-	-	-	-	-
P#4	385	176.0	-	130.3	-	-	-	-	-	-
CLDa	379	156.7	30.7	129.2	28.0	133.8	161.8	0.96	79	17
CLDb	391	188.9	33.9	131.2	31.0	136.2	167.2			
CHDa	384	180.6	61.0	130.1	58.0	139.1	197.1	0.94	69	25
CHDb	387	227.0	46.0	129.8	43.0	136.6	179.7			
GLD	391	155.8	9.3	131.1	8.7	132.6	141.3	0.91	85	6
GHDa	384	179.5	18.3	129.6	17.2	132.4	149.6	0.92	82	10
GHDb	386	147.4	15.8	130.4	14.9	132.8	147.7			

Conclusions

The present paper reports a contribution to the development of reliable quantitative models for design of FRP diagonal layouts for shear strengthening of tuff masonry walls. Attention is paid to identify and quantify the shear contribution of FRP reinforcement and masonry. The problem is approached on experimental basis, since a number of relevant experimental tests have been carefully revisited comparing local and global response of the specimens.

To this end, a truss model combined with the Turnšek and Căčovič's shear strength model is proposed. The results showed that: (a) The FRP strain values and hence the tensile force transmitted along the diagonal reinforcement show a nonlinear behavior; (b) the proposed truss model combined with the shear strength formula of Turnšek and Căčovič provides satisfactory results compared with the experimental data. A refined numerical analysis would still be advantageous to provide further insight into the synergistic interactions of FRP and masonry when proper anchorage of the shear reinforcement is ensured.

References

ACI 440.7R-10: Guide for the Design and Construction of Externally Bonded FRP Systems for Strengthening Concrete Structures. Reported by ACI Committee 440. Farmington Hills, Michigan, USA; 2010.

CNR-DT 200/2004: Guide for the Design and Construction of Externally Bonded FRP Systems for Strengthening Existing Structures. CNR - National Research Council, Rome, Italy, 2008, http://www.cnr.it.

Db Murature Unina-Dist. Raccolta dei Dati Esistenti sui Parametri Meccanici ed Elastici delle Murature. Progetto esecutivo RELUIS 2005/2008, 2009 (www.reluis.unina.it).

Magenes 1997: Magenes, G., G.M. Calvi, "In-plane Seismic Response of Brick Masonry Walls," Earthquake Engineering and Structural Dynamics, 26, 1997, pp. 1091-1112.

Marcari 2007: Marcari, G., G. Manfredi, A. Prota, M. Pecce, "In-plane Shear Performance of Masonry Panels Strengthened with FRP," Composite Part B, 38, 2007, pp. 887-901.

NTC 08: Norme tecniche per le costruzioni (Italian Technical Code for the design of constructions). D.M. 14/1/2008, Official Bullettin no. 29 of February 4 2008 (In Italian).

Prota 2008: Prota, A., G. Manfredi, F. Nardone, "Assessment of Design Formulas for in-plane FRP Strengthening of Masonry Walls," Journal of Composites for Construction (ASCE), 12(6), 2008, pp. 643-649.

Stratford 2004: Stratford, T., G. Pascale, O. Manfroni, B. Bonfiglioli, "Shear Strengthening Masonry Panels with Sheet Glass-Fiber Reinforced Polymer," Journal of Composites for Construction (ASCE), 8(5), 2004, pp. 434-443.

Turnšek 1971: Turnšek, V., F. Căčovič, "Some Experimental Results on the Strength of Brick Masonry Walls," Proceedings to 2nd International Brick Masonry Conference, Stoke-on-Trent, U.K., 1971, pp. 149-156.

Zhao 2003: Zhao, T., CJ. Zhang, J. Xie, "Experimental Study on Earthquake Strengthening of Brick Walls with Continuos Carbon Fibre Sheet," Masonry International,16(1), 2003, pp. 21-25.